Application of XLENS® program to neutron diffraction data: solving crystal structures with positive and negative scatterers

J. Rius, C Frontera*, C. Miravitlles
Institut de Ciència de Materials de Barcelona-CSIC, Campus Universitari de Bellaterra, 08193 Bellaterra, Catalonia, Spain

Abstract. Direct methods based on the origin-free modulus sum function (*S*) were first adapted in 1994 to the processing of intensity data from density functions with positive and negative scatterers. Nevertheless, that implementation used phase relationships explicitly with the inherent limitation introduced by the time consuming manipulation of quartets. This limitation was removed with the introduction of the *S*-FFT algorithm (maximising *S* with only Fourier transforms) and its posterior adaptation S_2-FFT for non-positive definite density functions. In the present work both algorithms are reformulated into a generalized one, thus simplifying their implementation in the XLENS® program. The resulting unified *S*-FFT algorithm is highly effective for crystal structures with at least one medium-heavy scatterer in the unit cell. We have successfully applied it on neutron diffraction data of compounds with negative Fermi lengths.

1. Introduction

XLENS® is a computer program intended to solve crystal structure from diffraction data by applying first principles (direct methods) to the measured intensities. This is achieved by optimizing the origin-free modulus sum function, $S(\Phi)$, in terms of the Φ subset of $\varphi_{\mathbf{h}}$ phases of the **h** strong reflections [1]. Initially, $S(\Phi)$ was expressed as a function of triple-phase relationships (triplets) and hence could only handle positive definite density functions. The use of triplets made the phase refinements time-consuming. Even more computing-time demanding was the adaptation of $S(\Phi)$ to density functions with positive and negative scatterers, since in this latter case four-phase relationships (quartets) were required [2]. To overcome this limitation, the algorithm was modified to replace the need of triplets/quartets by the use of the Fast Fourier Transform (FFT) subroutine. The resulting *S*-FFT algorithm was developed in Ref [3] and extended later (S_2-FFT) to density functions with positive and negative scatterers in Refs. [4,5]. At present these are the algorithms implemented in XLENS®.

In the present contribution the description of the S-FFT and S_2-FFT algorithms is unified by making use of the recently introduced $\delta(\boldsymbol{r})$ function [6]

$$\delta(\boldsymbol{r}) = \frac{1}{V}\sum_{\mathbf{H}}(E_{\mathbf{H}} - \langle E\rangle)\cdot e^{i\alpha_{\mathbf{H}}}\cdot e^{-i2\pi\mathbf{H}\boldsymbol{r}} \qquad (1)$$

which has been demonstrated to be essentially equivalent to the density function

$$\rho(\boldsymbol{r}) = \frac{1}{V}\sum_{\mathbf{h}} E_{\mathbf{h}}\cdot e^{i\varphi_{\mathbf{h}}}\cdot e^{-i2\pi\mathbf{h}\boldsymbol{r}} \qquad (2)$$

where $E_{\mathbf{h}}$ and $\varphi_{\mathbf{h}}$ are, respectively the amplitude and the associated phase of the quasi-normalized structure factor. The E values can be derived from the corresponding experimental structure factor amplitudes F by means of $E_{\mathbf{h}} = F_{\mathbf{h}}/\sum_j f_j^2$ where f_j is the atomic scattering factor for atom j in the

unit cell with *N* atoms (for the case of neutrons, Fermi length of nuclei must be used). If $\rho(\boldsymbol{r})$ is positive definite the relation between both is

$$\rho(\boldsymbol{r}) \cong k \cdot \delta(\boldsymbol{r}) \cdot m(\boldsymbol{r}) \quad (3)$$

with *k* being a suitable scaling constant and with the $m(\boldsymbol{r})$ mask taking only the values one or zero depending if the value of $\delta(\boldsymbol{r})$ is above or below the experimental threshold limit defined by $t \cdot \sigma(\delta)$ with t= 2.5. The $\alpha_{\mathbf{H}}$ phase values in (1) are estimated from the *N* highest peaks found in $\delta(\boldsymbol{r}) \cdot m(\boldsymbol{r})$. The new structure factor estimate $\boldsymbol{E}_{\mathbf{H}}$ is then given by

$$\boldsymbol{E}_{\mathbf{H},\text{new}} = E_{\mathbf{H}} \cdot e^{i\varphi_{\mathbf{H}}} = \frac{k}{V}\int_V \delta(\boldsymbol{r}) \cdot m(\boldsymbol{r}) \cdot e^{i2\pi \mathbf{H}\boldsymbol{r}} d\boldsymbol{r} \quad (4)$$

The recursive application of (4) is the basis of the δ recycling phase-refinement procedure [7].

2. The S-FFT algorithm for positive-definite ρ functions:

Let the $\rho(\boldsymbol{r})$ density function be peaked at the atomic positions. This means that ρ and the corresponding squared density function ρ^{sq} are proportional. By multiplying both sides of (3) with $\rho(\boldsymbol{r})$, it follows

$$\rho^{sq}(\boldsymbol{r}) \cong k \cdot \rho(\boldsymbol{r}) \cdot \delta(\boldsymbol{r}) \cdot m(\boldsymbol{r}) \quad (5)$$

The structure factors of ρ^{sq} may be approximated by

$$\boldsymbol{E}^{\boldsymbol{sq}}_{\mathbf{h},\text{new}} = \frac{k}{V}\int_V \delta(\boldsymbol{r}) \cdot \rho(\boldsymbol{r}) \cdot e^{i2\pi \mathbf{h}\boldsymbol{r}} d\boldsymbol{r} \quad (6)$$

because the mask can be set equal to 1 in the whole unit cell due to the positivity. In view of the proportionality of ρ^{sq} and ρ, the new phase estimates of ρ can be obtained from

$$\boldsymbol{E}_{\mathbf{h},\text{new}} = E_{\mathbf{h},\text{new}} \cdot e^{i\varphi_{\mathbf{h},\text{new}}} \propto \boldsymbol{E}^{\boldsymbol{sq}}_{\mathbf{h},\text{new}} \quad (7)$$

which is only valid for the subset of large **h** reflections. The $\alpha_{\mathbf{H}}$ phase values associated with $\delta(\boldsymbol{r})$ are obtained from $\rho(\boldsymbol{r})^2$, i.e. from squaring the values of the $\rho(\boldsymbol{r})$ synthesis computed with the **h** reflections, only. Since no atomic peaks need be identified, no peak search subroutine is necessary.

3. The S-FFT algorithm for sign-unrestricted ρ functions

In the case of ρ functions with positive and negative peaks, it is convenient to introduce a new mask fulfilling the following criterion [4,5]:

$$\begin{aligned} m(\mathbf{r}) &= 1 \quad \text{if } \rho(\mathbf{r}) > t\,\sigma(\rho) \quad (8)\\ &= -1 \quad \text{if } \rho(\mathbf{r}) < -t\,\sigma(\rho)\\ &= 0 \quad \text{if } -t\,\sigma(\rho) < \rho(\mathbf{r}) < t\,\sigma(\rho) \end{aligned}$$

where **r** ranges over the whole unit cell and with *t* being close to 2.5. This mask allows introducing a new density function called $\rho^{sq-s}(\boldsymbol{r})$ where *sq-s* stand for "squared-shaped". This new function results from the product of $\rho^{sq}(\boldsymbol{r}) \cdot m(\boldsymbol{r})$ and has the same peak shapes than $\rho^{sq}(\boldsymbol{r})$ but the same peak signs as $\rho(\boldsymbol{r})$. In other words, $\rho^{sq-s}(\boldsymbol{r})$ and $\rho(\boldsymbol{r})$ are proportional. By multiplying both sides of (3) with $\rho(\boldsymbol{r}) \cdot m(\boldsymbol{r})$, it follows

$$\rho^{sq-s}(\boldsymbol{r}) \cong k \cdot \rho(\boldsymbol{r}) \cdot \delta(\boldsymbol{r}) \cdot m(\boldsymbol{r}) \quad (9)$$

with the structure factors of $\rho^{sq-s}(\boldsymbol{r})$ being

$$\boldsymbol{E}^{sq-s}_{\mathbf{h},new} = \frac{1}{V}\int_V \delta(\boldsymbol{r}) \cdot \rho(\boldsymbol{r}) \cdot m(\boldsymbol{r}) \cdot e^{i2\pi \mathbf{h}\boldsymbol{r}} d\boldsymbol{r} \quad (10)$$

Due to the proportionality of ρ^{sq-s} and ρ, the new phase estimates of ρ can be obtained from

$$\boldsymbol{E}_{\mathbf{h},\text{new}} = E_{\mathbf{h},\text{new}} \cdot e^{i\varphi_{\mathbf{h},\text{new}}} \propto \boldsymbol{E}^{\boldsymbol{sq-s}}_{\mathbf{h},\text{new}} \quad (11)$$

which only holds for the subset of large **h** reflections. The α_H phase values associated with $\delta(\boldsymbol{r})$ are obtained by squaring the values of the $\rho(\boldsymbol{r})$ synthesis computed with only the **h** reflections followed by multiplication with $m(\mathbf{r})$.

4. The unified *S*-FFT algorithm

Figure 1 shows the flow chart of the S-FFT algorithm in its unified version. Definition of the mask **m** is in accordance to the type of problem being treated: It takes values 1 or 0 (for ρ above or below the threshold limit, respectively) in the case of positive scatterers, or it is defined by (8) in the case of positive and negative scatterers. A slight modification of *m* was shown to be more effective in the case of light scatterers [5]

$$\begin{aligned} m(\mathbf{r}) &= 1 \quad \text{if } \rho(\mathbf{r}) > t\,\sigma(\rho) \\ &= -1 \quad \text{if } \rho(\mathbf{r}) < -t\,\sigma(\rho) \\ &= a \quad \text{if } -t\,\sigma(\rho) < \rho(\mathbf{r}) < t\,\sigma(\rho) \end{aligned} \qquad (12)$$

where *a* is a random number between -1 and 1. Nevertheless, this modification was tested for solving organic compounds from X-ray diffraction data but not for solving structures from neutron data. In the following section we have tested this new mask for two examples from neutron diffraction.

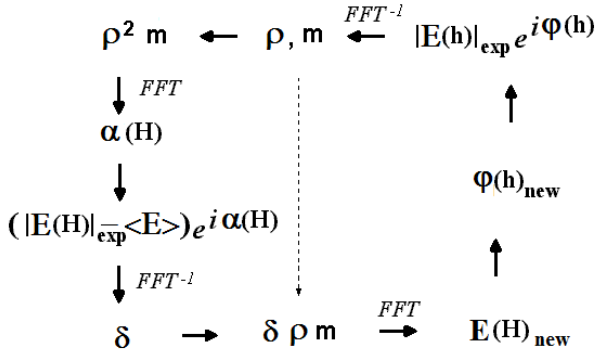

Figure 1

The unified *S*-FFT phase refinement procedure. The initial phases (upper right corner) are combined with the experimental amplitudes to compute the electron density ρ and the associate mask m. The mask is used to compute the phases α of the δ function and also (broken arrow) the product function, $\delta \cdot \rho \cdot m$. The Fourier transform of this product function yields the new structure factor estimates.

5. Results of test structure solutions from neutron diffraction.

5.1. $Bi_{0.75}Sr_{0.25}MnO_3$

We have used S-FFT implemented in XLENS® (option MASK=-2) to find negative neutron scatterers in two different examples of well known structures. The first example consists on its application to a perovskite compound with unit formula $(Bi_{0.75}Sr_{0.25})MnO_3$ containing the strong negative neutron scatterer Mn [8]. Fermi lengths for Bi, Sr, Mn and O are, respectively, 0.853, 0.702, -0.373, 0.580 fm and the crystal data are *a*= 5.499, *b*= 7.770, *c*= 5.542 Å, space group: *I mma*, *Z*= 4. We have used in the calculations the intensities extracted from the observed powder diffraction pattern (measured at D2B) by redistributing the global intensities of the overlapped peaks according to the calculated individual intensities. After 50 trials (starting with random phases), the program reports the true structure for 7 sets of initial values. These right solutions are easily identifiable for their low values of the residual. Table 1 lists the peaks in the E-map. Bond distances found directly from the structural resolution are listed and compared with those reported in Ref. [8] as a test for the accuracy of the peak finding.

Table 1. Application of the unified *S*-FFT algorithm to neutron diffraction data. Compound data: a=5.499, b= 7.770, c=5.542 space group: *I mma*, Unit formula: $(Bi_{0.75}Sr_{0.25})MnO_3$, Z=4. Success rate 3/25. All atoms with absolute relative height greater than 90 are listed. Bond distances found are compared with those reported from the refinement of NPD data [8].

Atom	rel. height	x/a	y/b	z/c	Site	Bond distances(Å)	
Bi,Sr	1000	0	¼	0.9974	4e	Found/Reported	
Mn	-579	½	0	0	4b	Mn-O1	⟨Mn-O2⟩
O1	474	½	¾	0.0501	4e	1.962	1.964
O2	409	¼	0.0275	¼	8g	1.9690(9)	1.9704(6)

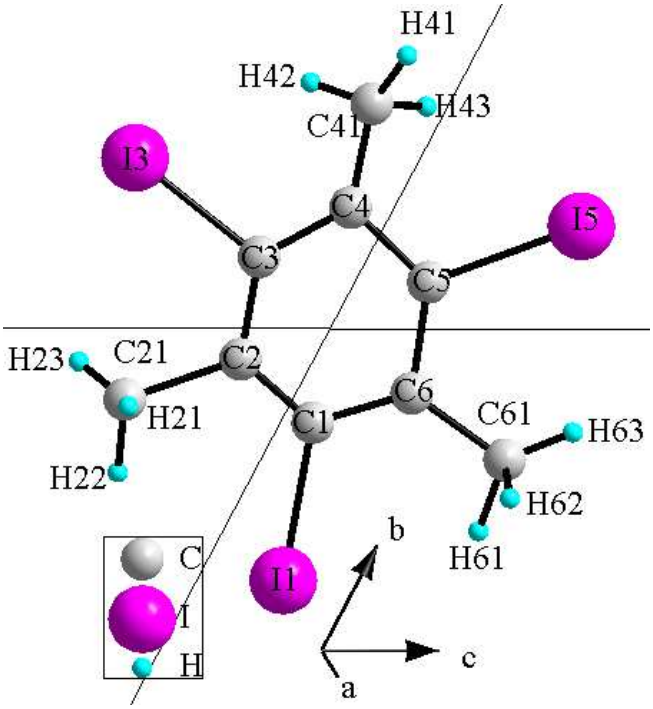

Figure 2:
Graphical view of the C9H9I3 compound from the peak positions found by application of extended S_2-FFT procedure implemented in XLENS®.

Table 2
C-H bond distances (in Å) as found compared to that refined in Ref. [9].

Bond	Found	Report.
C21-H21	0.952	1.068(4)
C21-H22	1.176	1.076(4)
C21-H23	0.853	1.068(4)
C41-H41	1.066	1.077(3)
C41-H42	0.911	1.059(5)
C41-H43	1.057	1.046(5)
C61-H61	1.173	1.081(4)
C61-H62	0.973	1.085(4)
C61-H63	0.958	1.044(4)

5.2. $C_9H_9I_3$

The second test example is the application of XLENS® to the single-crystal neutron diffraction data of the 1,3,5-triiodo-2,4,6-trimethylbenzene (TIM) molecule. The single-crystal neutron diffraction study of this molecule was published by [9]. The neutron intensities were collected at 15 K on the D9 four-circle diffractometer at the high-flux reactor of ILL (Grenoble, France). The monochromator was a copper single-crystal selecting the (2 2 0) reflection giving λ= 0.70379 Å. Crystal data: *a* = 7.905, *b* = 9.510, *c* = 9.521 Å, α= 60.41, β= 66.64, γ= 86.24º, *V*= 563.7A3, space group *P*-1, molecular formula: $C_9H_9I_3$, *Z*= 2, crystal dimensions: 4 x 2 x 1 mm^3. Due to detector problems only 2071 reflections could be measured (-4< h <8, -9< k <9, -9< l <9). Averaging of the equivalent data gave 1079 independent reflections. The Fermi lengths for C, I and H are, respectively, 0.665, 0.528 and -0.374. The

parameters defining the direct methods *S* phase refinement function are: <E> = 1.073, d_{min}=0.82, E_{ratio}=0.92, strongest E value = 3.46, lowest large E value= 1.35, number of sets: 100, maximum number of cycles: 39. Phase refinement with *S*-FFT in *P*1 always gives the correct solution. The subsequent automated finding of the symmetry centre is successful in 30% of the cases. The structure found is depicted in Fig. 2 and it is in very good accordance with the refined structure (Fig. 7 in Ref. [9]). Bond distances found directly from the structural resolution are listed in Table 2 and compared with those reported from the structural refinement.

6. Conclusions

The introduction of mask m(**r**) (8) or (12) in the procedure depicted in Fig. 1 allows the proper finding of negative scatterers. To prove it and show its applicability to the solution of structures containing nuclei with negative Fermi lengths, we have used XLENS® in two case examples and successfully found Mn (in the first) and H (in the second). The comparison of bond distances with those reported prove that the positions found for negative scatterers are accurate enough and can be taken as a good starting point for subsequent structural refinement. This proves the utility of this implementation for solving structures from neutron diffraction.

Acknowledgments

The authors thank the Spanish 'Ministerio de Ciencia e Innovación' (projects MAT2009-07967 and Consolider NANOSELECT CSD2007-00041) and the 'Generalitat de Catalunya' SQR(2009) for financial support. The authors want to express their gratitude to Dr. Mª Teresa Fernández-Díaz for kindly supplying the single-crystal neutron diffraction data.

References

[1] Rius J, 1993, Acta Cryst. A**49**, 406.
[2] Rius J, Miravitlles C, Allman R, 1996, Acta Cryst. A**52**, 634.
[3] Rius J, Crespi A, Torrelles X, 2007, Acta Cryst. A**63**, 131.
[4] Rius J, Frontera C, 2008, Acta Cryst. A**64**, 670.
[5] Rius J, Frontera C, 2009, Acta Cryst. A**65**, 528.
[6] Rius J, 2012, Acta Cryst. A**68**, 77.
[7] Rius J, 2012, Acta Cryst. A**68**, 399.
[8] Frontera C, García-Muñoz J L, Aranda M A G, Hervieu M, Ritter C, Mañosa L, Capdevila X G, Calleja A, 2004, Phys. Rev. B **68**, 134408
[9] Boudjada A, Meinnel J J, Boucekkine A, Hernandez O J, Fernández-Díaz M T, 2002, J. Chem. Phys. **117**, 10173.